



ELSEVIER

Contents lists available at ScienceDirect

Physica E

journal homepage: [www.elsevier.com/locate/physa](http://www.elsevier.com/locate/physa)

# Influence of phonon confinement on the optically-detected electrophonon resonance line-width in cylindrical quantum wires

Le Thi Thu Phuong<sup>a,b,\*</sup>, Huynh Vinh Phuc<sup>c</sup>, Tran Cong Phong<sup>b</sup>

<sup>a</sup> Department of Physics, Hue University's College of Education, No. 34, Le Loi Str., Hue City, Viet Nam

<sup>b</sup> Center for Theoretical and Computational Physics, Hue University's College of Education, No. 34, Le Loi Str., Hue City, Viet Nam

<sup>c</sup> Department of Physics, Dong Thap University, No. 783, Pham Huu Lau Str., Dong Thap, Viet Nam

## HIGHLIGHTS

- Absorption power is calculated taking into account the phonon confinement effect.
- Optically detected electrophonon resonance line-width (ODEPRLW) as profiles of curves is determined.
- The ODEPRLW increases with increasing temperature and decreases with increasing wire's radius.
- The ODEPRLW in the case of confined phonons is greater than it is in the case of bulk phonons.
- The influence of phonon confinement is very small and can be neglected for wires with large radii.

## ARTICLE INFO

### Article history:

Received 7 April 2013

Received in revised form

2 August 2013

Accepted 19 August 2013

Available online 29 August 2013

### Keywords:

Line-width

Absorption power

Cylindrical quantum wire

Optically-detected electrophonon resonance

## ABSTRACT

We investigate the effect of phonon confinement on the optically-detected electrophonon resonance (ODEPR) effect and ODEPR line-width in cylindrical quantum wires. The ODEPR conditions as functions of the wire's radius and the photon energy are also obtained. The shifts of ODEPR peaks caused by the confined phonon are discussed. The numerical result for the GaAs/AlAs cylindrical quantum wire shows that in the two cases of confined and bulk phonons, the line-width (LW) decreases with increasing wire's radius and increases with increasing temperature. Furthermore, in the small range of the wire's radius ( $R \leq 30$  nm) the influence of phonon confinement plays an important role and cannot be neglected in reaching the ODEPR line-width.

© 2013 Elsevier B.V. All rights reserved.

## 1. Introduction

The absorption line-width (LW) is well-known as a good tool for investigating the scattering mechanisms of carriers and, hence, can be used to probe electron–phonon scattering processes. To investigate the effects of various scattering processes, absorption line-widths (LWs) have been measured in various kinds of semi-conductors, such as quantum wells [1–6], quantum wires [7–10], and quantum dots [11–15]. These results show that the absorption LW has a weak dependence on temperature and has a strong dependence on system size. However, in those articles, the absorption LW was investigated based on the interaction of electrons and bulk phonons, the absorption LW in cylindrical

quantum wires (CQWs) due to the confined-LO-phonon–electron interaction is still open for study.

A CQW is formed by a cylindrical wire of material one (such as GaAs) whose length is very much larger than radius, embedded in material two where the band-gap is much larger than it is in material one (such as AlGaAs). Carriers are confined in material one where the potential well develops by the band-gap difference between two materials. In this structure, phonon confinement is an essential part of the description of electron–phonon interactions [16]. It causes the increase of electron–phonon scattering rates [17–19] and significant nonlinearities in the dispersion relations of acoustic-phonon modes, and modifies the phonon density of states [20]. The polaronic states may be affected by changes in the Frohlich Hamiltonian caused by phonon confinement [21]. Since the early experimental observations of confined phonons [22,23], phonon modes in low-dimensional structures have been attracting much attention [16,24]. There have been many models dealing theoretically with phonon modes, such as

\* Corresponding author at: Department of Physics, Hue University's College of Education, No. 34, Le Loi Str., Hue City, Viet Nam. Tel.: +84 979515588.

E-mail address: [thuphuonghueuni@gmail.com](mailto:thuphuonghueuni@gmail.com) (L. Thi Thu Phuong).

the hybridization theory, the Huang-Zhu model, the dielectric continuum model (see Ref. [21] and references therein). Phonon confinement is shown to be important whenever the transverse dimensions of a quantum wire are smaller than the phonon coherence length [16] and should be taken into account in order to obtain realistic estimates for electron–phonon scattering in low-dimensional structures [25–27]. Phonon confinement affects the optically-detected electrophonon resonance (ODEPR) effect mainly through changes in the selection rules for transitions involving subband electrons, and affects the ODEPR line-width (ODEPRLW) through changes in the probability of electron–phonon scattering. The LW is defined by the profile of curves describing the dependence of the absorption power (AP) on the photon energy or frequency [28,29]. Recently, our group has proposed a method, called the profile method, to computationally obtain the LW from graphs of the AP [30], and we used this method to determine the cyclotron resonance LW in CQWs [31] and in GaAs/AlAs quantum wires [32].

In the present work, we investigate the intersubband ODEPRLW in a CQW. We study the dependence of the ODEPRLW on the wire's radius and the temperature of system. The results of the present work are fairly different from the previous results because the phonon confinement is taken into account and because the results can be applied to optically detect the resonant peaks. The paper is organized as follows: calculations of analytic expression of the AP in CQWs taking into account the phonon confinement effect are presented in Section 2. The graphic dependence of the AP on the photon energy in the GaAs/AlAs CQW is shown in Section 3. From this dependence, we obtain the LW and examine the dependence of the LW on temperature and wire's radius. Finally, remarks and conclusions are shown briefly in Section 4.

## 2. Absorption power in a cylindrical quantum wire

Let us consider a cylindrical GaAs wire of radius  $R$  and length  $L$  ( $L \gg R$ ) embedded in AlAs. Under the infinitely deep well approximation, the electron wave function can be written as [33]

$$\Psi_{\ell j, k_z}(\vec{r}) = \frac{e^{ik_z z}}{\sqrt{L}} D_{\ell j} J_{\ell}(x_{\ell j} \frac{r}{R}) e^{i\ell\phi}, \quad (1)$$

with the corresponding energy

$$E_{\ell j}(k_z) = \frac{\hbar^2 k_z^2}{2m_e} + \frac{\hbar^2 (x_{\ell j})^2}{2m_e R^2}, \quad (2)$$

where  $\ell = 0, \pm 1, \pm 2, \dots$ ,  $j = 1, 2, 3, \dots$ ,  $\vec{r} = (r, \phi, z)$  are the cylindrical coordinates for the system and  $k_z$  denotes the axial wave-vector component.  $D_{\ell j} = 1/(\sqrt{\pi} y_{\ell j} R)$  is the normalization factor,  $x_{\ell j}$  is the  $j$ th zero of the  $\ell$ th order Bessel function, i.e.,  $J_{\ell}(x_{\ell j}) = 0$  and  $y_{\ell j} = J_{\ell+1}(x_{\ell j})$ , and  $m_e$  is the effective mass of electron.

When an electromagnetic wave characterized by the time-dependent electric field of amplitude  $E_0$  and angular frequency  $\omega$  is applied to this system along the  $r$ -direction, the AP delivered to the system,  $P(\omega)$ , is given by [34]

$$P(\omega) = (E_0^2/2) \text{Re}\{\sigma_r(\omega)\}, \quad (3)$$

where “Re” denotes “the real part of”,  $\sigma_r(\omega)$  is the  $r$ -component of the optical conductivity tensor. This component can be written further in a tangible form using the projection method on the linear response scheme as [35,36]

$$\text{Re}\{\sigma_r(\omega)\} = e^2 \sum_{\alpha, \beta} |J_r^{\alpha\beta}| |r_{\alpha\beta}| \frac{(f_{\beta} - f_{\alpha}) \gamma_{\alpha\beta}(\omega)}{[\hbar\omega - (E_{\beta} - E_{\alpha})]^2 + [\gamma_{\alpha\beta}(\omega)]^2}, \quad (4)$$

here  $e$  is the charge of a conduction electron,  $E_{\alpha} \equiv E_{\ell_{\alpha} j_{\alpha}}(k_z^{\alpha})$  and  $E_{\beta} \equiv E_{\ell_{\beta} j_{\beta}}(k_z^{\beta})$  are the energies of the initial and the final states,

$f_{\alpha} \equiv f(\ell_{\alpha}, j_{\alpha}, k_z^{\alpha})$  being the Fermi–Dirac distribution function for an electron at the state  $|\alpha\rangle$ ,  $r_{\alpha\beta}$  and  $J_r^{\alpha\beta}$  are the matrix elements of the position operator and the current operator, respectively, given by

$$|r_{\alpha\beta}| = \langle \alpha | r | \beta \rangle = \frac{(2\pi)^2}{\pi R^2 L} \delta_{k_z^{\beta}, k_z^{\alpha}} \delta_{\ell_{\alpha}, \ell_{\beta}} N_{\ell_{\alpha} j_{\alpha}, \ell_{\beta} j_{\beta}}(R), \quad (5)$$

$$|J_r^{\alpha\beta}| = \left| \left\langle \alpha, k_z^{\alpha} \left| \frac{ie\hbar}{m_e} \frac{\partial}{\partial r} \right| \beta, k_z^{\beta} \right\rangle \right| = \frac{4i\pi e\hbar}{m_e R^2 L} \delta_{k_z^{\beta}, k_z^{\alpha}} \delta_{\ell_{\alpha}, \ell_{\beta}} M_{\ell_{\alpha} j_{\alpha}, \ell_{\beta} j_{\beta}}(R). \quad (6)$$

In these expressions, it is difficult to determine the explicit forms of the matrix elements  $N_{\ell_{\alpha} j_{\alpha}, \ell_{\beta} j_{\beta}}(R)$  and  $M_{\ell_{\alpha} j_{\alpha}, \ell_{\beta} j_{\beta}}(R)$  for arbitrary states. So, in the following calculation we will only make use of the radial wave function for the ground state employed recently by Masale and Constantinou [37] and Gold and Ghazali [38]. The component  $\gamma_{\alpha\beta}(\omega)$  in Eq. (4) is called the damping term [35,36] and is given by the following equation:

$$\begin{aligned} \gamma_{\alpha\beta}(\omega) &= (f_{\beta} - f_{\alpha}) \\ &= \pi \sum_{\mu, q} |C_{\beta\mu}(q)|^2 \left\{ [(1 + N_q) f_{\alpha}(1 - f_{\mu}) \right. \\ &\quad - N_q f_{\mu}(1 - f_{\alpha})] \delta(\hbar\omega - E_{\mu} + E_{\alpha} - \hbar\omega_q) \\ &\quad + [N_q f_{\alpha}(1 - f_{\mu}) - (1 + N_q) f_{\mu}(1 - f_{\alpha})] \delta(\hbar\omega - E_{\mu} + E_{\alpha} + \hbar\omega_q) \left. \right\} \\ &\quad + \pi \sum_{\mu, q} |C_{\alpha\mu}(q)|^2 \left\{ [(1 + N_q) f_{\mu}(1 - f_{\beta}) \right. \\ &\quad - N_q f_{\beta}(1 - f_{\mu})] \delta(\hbar\omega - E_{\beta} + E_{\mu} - \hbar\omega_q) \\ &\quad + [N_q f_{\mu}(1 - f_{\beta}) - (1 + N_q) f_{\beta}(1 - f_{\mu})] \delta(\hbar\omega - E_{\beta} + E_{\mu} + \hbar\omega_q) \left. \right\}, \quad (7) \end{aligned}$$

where  $\delta(\dots)$  is the Dirac's delta function;  $N_q$  is the Planck distribution function for a phonon in the state  $|q\rangle = |m, n, q_z\rangle$ ;  $\omega_q^2 = \omega_0^2 - \gamma^2(q_{mn}^2 + q_z^2)$  where  $\omega_0$ ,  $\gamma$ ,  $q_z$  are, respectively, the zone-center LO phonon frequency, the velocity parameter ( $4.73 \times 10^3 \text{ m s}^{-1}$  for GaAs [39]), the wave vector of phonon along the wire axis; and  $C_{\beta\mu}(q)$  is the matrix elements of electron–phonon interaction and depends on the scattering mechanism. In this model, it is given by

$$C_{\beta\mu}(q) = C_{mn}(q_z) I_{\ell_{\beta} j_{\beta}, \ell_{\mu} j_{\mu}}(q_{mn}) \delta_{k_z^{\beta}, k_z^{\mu} + q_z}, \quad (8)$$

where [33,40]

$$I_{\ell_{\beta} j_{\beta}, \ell_{\mu} j_{\mu}}(q_{mn} R) = 2 \int_0^1 \xi d\xi \frac{1}{y_{\ell_{\beta} j_{\beta}} y_{\ell_{\mu} j_{\mu}}} J_{\ell_{\beta}}(x_{\ell_{\beta} j_{\beta}} \xi) J_{\ell_{\mu}}(x_{\ell_{\mu} j_{\mu}} \xi) J_{|\ell_{\beta} - \ell_{\mu}|}(q_{mn} R \xi) J_{\ell_{\mu}}(x_{\ell_{\mu} j_{\mu}} \xi), \quad (9)$$

$$|C_{mn}(q_z)|^2 = \frac{\pi e^2 \hbar \omega_0}{2V J_{m+1}^2(x_{mn})} \left( \frac{1}{\chi_{\infty}} - \frac{1}{\chi_0} \right) \frac{1}{q_{mn}^2 + q_z^2}, \quad (10)$$

with  $q_{mn} R = x_{mn}$  [41],  $V = \pi R^2 L$  is the volume of the quantum wire,  $\chi_0$  and  $\chi_{\infty}$  are the static and high-frequency dielectric constants, respectively.

To obtain a detailed expression for the AP, we need to calculate  $\gamma_{\alpha\beta}(\omega)$  in Eq. (7) and then substitute it into Eqs. (4) and (3). To do this, we change the summations over  $q$  and  $\mu$  into integrals as

$$\sum_q \rightarrow \frac{L}{2\pi} \sum_{m,n} \int_{-\infty}^{+\infty} dq_z, \quad \sum_{\mu} \rightarrow \frac{L}{2\pi} \sum_{\ell_{\mu} j_{\mu}} \int_{-\infty}^{+\infty} dk_z^{\mu}. \quad (11)$$

Also, the power absorption in the system for the transition between the two lowest sublevels is simply calculated at the band edge ( $k_z^{\alpha} = 0$ ). Note that the selection rule requires  $k_z^{\alpha} = k_z^{\beta}$  or a direct transition. After some mathematical manipulation, we have

$$\begin{aligned} \gamma_{\alpha\beta}(\omega) &= [f_{\beta} - f_{\alpha}] \\ &= \sum_{\ell_{\mu} j_{\mu}, m, n} \sum_{\ell_{\beta} j_{\beta}} \left\{ \frac{|I_{\ell_{\mu} j_{\mu}, \ell_{\beta} j_{\beta}}|^2}{(Q_1^2 + q_{mn}^2) Y^{(-)}(Q_1, q_{mn})} \right. \\ &\quad \times \left. \left[ (1 + N_q) f_{\ell_{\alpha} j_{\alpha}, 0} (1 - f_{\ell_{\mu} j_{\mu}, Q_1}) - (1 + N_q) f_{\ell_{\mu} j_{\mu}, Q_1} (1 - f_{\ell_{\alpha} j_{\alpha}, 0}) \right] \right\} \end{aligned}$$

$$\begin{aligned}
& + \frac{|I_{\ell_{\mu j_{\mu}} \ell_{\beta j_{\beta}}}|^2}{(Q_1^2 + q_{mn}^2) Y^{(+)}(Q_1, q_{mn})} \\
& \times \left[ N_q f_{\ell_{\alpha j_{\alpha}, 0}} (1 - f_{\ell_{\mu j_{\mu}, Q_1}}) - (1 + N_q) f_{\ell_{\mu j_{\mu}, Q_1}} (1 - f_{\ell_{\alpha j_{\alpha}, 0}}) \right] \\
& + \frac{|I_{\ell_{\alpha j_{\alpha}} \ell_{\mu j_{\mu}}}|^2}{(Q_2^2 + q_{mn}^2) Y^{(+)}(Q_2, q_{mn})} \\
& \times \left[ (1 + N_q) f_{\ell_{\mu j_{\mu}, Q_2}} (1 - f_{\ell_{\beta j_{\beta}, 0}}) - N_q f_{\ell_{\beta j_{\beta}, 0}} (1 - f_{\ell_{\mu j_{\mu}, Q_2}}) \right] \\
& + \frac{|I_{\ell_{\alpha j_{\alpha}} \ell_{\beta j_{\beta}}}|^2}{(Q_2^2 + q_{mn}^2) Y^{(-)}(Q_2, q_{mn})} \\
& \times \left[ N_q f_{\ell_{\mu j_{\mu}, Q_2}} (1 - f_{\ell_{\beta j_{\beta}, 0}}) - (1 + N_q) f_{\ell_{\beta j_{\beta}, 0}} (1 - f_{\ell_{\mu j_{\mu}, Q_2}}) \right] \Big\}, \quad (12)
\end{aligned}$$

where

$$\begin{aligned}
Y^{\pm}(Q_i, q_{mn}) &= \left| \frac{\hbar^2 \gamma^2}{(\omega_0^2 - \gamma^2 (q_{mn}^2 + Q_i^2))^{1/2} \pm \frac{\hbar^2}{m_e}} \right|, \\
Q_1 &= [a_1 + (a_1^2 - b_1)^{1/2}]^{1/2}, \quad Q_2 = [a_2 - (a_2^2 - b_2)^{1/2}]^{1/2}, \\
a_i &= \frac{2m_e}{\hbar^2} (\hbar\omega - \Delta E_{\mu i} - m_e \gamma^2), \\
b_i &= \frac{4m_e^2}{\hbar^4} [(\hbar\omega - |\Delta E_{\mu i}|)^2 - \hbar^2 (\omega_0^2 - \gamma^2 q_{mn}^2)], \\
f_{\ell_{\mu j_{\mu}, Q_i}} &= \{1 + \exp[(E_{\ell_{\mu j_{\mu}}}(Q_i) - E_F)/(k_B T)]\}^{-1}, \\
E_{\ell_{\mu j_{\mu}}}(Q_i) &= \frac{\hbar^2 Q_i^2}{2m_e} + \frac{\hbar^2 (\chi_{\ell_{\mu j_{\mu}}})^2}{2m_e R^2}, \quad i = 1, 2, \quad (13)
\end{aligned}$$

with  $E_F$  being the Fermi level.

We can see that these analytical results appear very involved. However, physical conclusions can be drawn from graphical representations and numerical results, obtained from adequate computational methods.

### 3. Numerical results and discussion

The expression of  $\gamma_{\alpha\beta}(\omega)$  in Eq. (7) exhibits a resonant behavior due to the ODEPR condition

$$\hbar\omega \pm \Delta E_{\beta\alpha} \pm \hbar\omega_q = 0, \quad (14)$$

where  $\Delta E_{\beta\alpha} \equiv \Delta E_{\ell_{\beta j_{\beta}} \ell_{\alpha j_{\alpha}}} = E_{\beta} - E_{\alpha}$ . Eq. (14) is the ODEPR condition in quantum wires. This result is the same as Lee's result for a quantum wire with the Woods–Saxon potential [42] and in a quantum well [43]. For the projection method in present calculation, there are three electron states involved in  $\gamma_{\alpha\beta}(\omega)$ : the initial state  $|\alpha\rangle$ , the intermediate state  $|\mu\rangle$ , and the final state  $|\beta\rangle$ . This means that an electron at the initial state can move directly to the final state or to the intermediate state and then to the final state. When the ODEPR conditions are satisfied, in the course of scattering events electrons in the state  $|\ell_{\alpha, j_{\alpha}}\rangle$  can transit to another state  $|\ell_{\beta, j_{\beta}}\rangle$  by absorbing a photon of energy  $\hbar\omega$  during the absorption and/or emission of a confined LO-phonon of energy  $\hbar\omega_q$ . To clarify the obtained results we numerically evaluate the AP,  $P(\omega)$ , for a specific GaAs/AlAs CQW. The AP is considered to be a function of the photon energy. The parameters used in our computational evaluation are as follows [37]:  $\chi_{\infty} = 10.9$ ,  $\chi_0 = 13.1$ ,  $m_e = 0.067 \times m_0$  ( $m_0$  being the mass of free electron),  $\hbar\omega_0 = 36.25$  meV,  $E_F = 0.5 \times 10^{-18}$  J,  $E_0 = 5 \times 10^6$  V m $^{-1}$ , and  $L = 100$  nm. The following conclusions are obtained in the extreme quantum limit, where only the lowest subbands are occupied:  $|\ell_{\alpha, j_{\alpha}}\rangle = |\ell_{\mu, j_{\mu}}\rangle = |0, 1\rangle$ ,  $|\ell_{\beta, j_{\beta}}\rangle = |1, 1\rangle$ .

In Fig. 1, the dashed curve ( $R=16$  nm) corresponds to  $\Delta E_{1101} = 19.2259$  meV and to the energy of confined phonon  $\hbar\omega_q = 36.2469$  meV. From the graph we can see that each peak describes a different resonance. By using the computational method, we easily determine that from the left to the right the

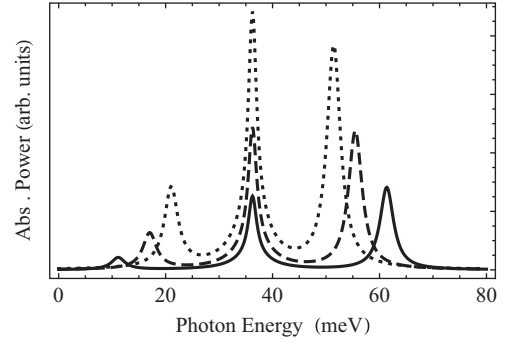


Fig. 1. Dependence of the AP on the photon energy for the different values of the wire's radius. The solid, the dashed and the dotted curves correspond to  $R=14$  nm,  $R=16$  nm and  $R=18$  nm, respectively. Here,  $T=300$  K.

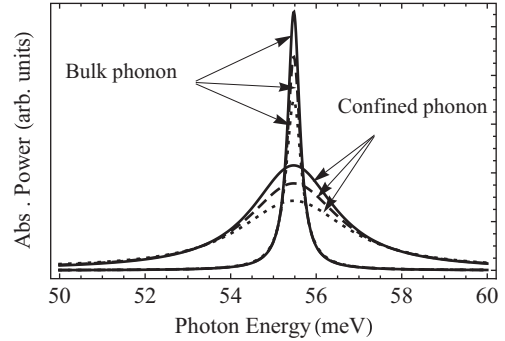
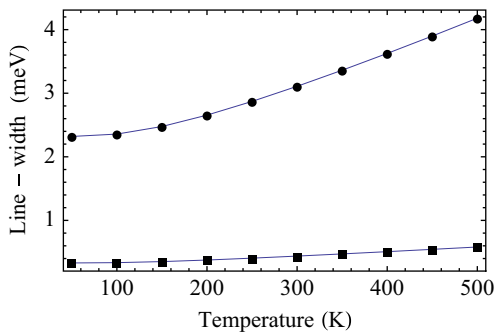


Fig. 2. The AP as a function of photon energy in the GaAs/AlAs CQW of  $R=16$  nm for three values of temperature: the solid, the dashed, and the dotted curves correspond to 100 K, 200 K, and 300 K, respectively.

first and the third peaks (of this curve) correspond to the values of the photon energy  $\hbar\omega^- = 17.0210$  meV and  $\hbar\omega^+ = 55.4728$  meV, respectively. They satisfy the ODEPR conditions  $\hbar\omega^{\mp} = \hbar\omega_q \mp \Delta E_{1101}$  ( $\hbar\omega^{\mp} = 36.2469 \mp 19.2259$  meV) and describe the inter-subband transitions of an electron from the initial state  $|0, 1\rangle$  to the final state  $|1, 1\rangle$  by absorbing (emitting) a phonon  $\hbar\omega_q$  and emitting (absorbing) a photon  $\hbar\omega^{\pm}$ . The second peak corresponds to the photon energy  $\hbar\omega^0 = 36.2469$  meV, satisfying the condition  $\hbar\omega^0 = \hbar\omega_q$ . This condition implies that an electron absorbs (emits) a photon along with emitting (absorbing) a phonon with the energy equals the photon energy so that energy of electron does not change. The cases of  $R=14$  nm (solid curve) and  $R=18$  nm (dotted curve) can be understood similarly. The ODEPR conditions give rise a possibility to determine the difference between energy levels experimentally by using an electromagnetic wave. In fact, from the figure and above ODEPR conditions we easily see that the first and the third peaks of each curve are always symmetrical to the second one and the distance between these two peaks (in the unit of energy) is always twice as much as  $\Delta E_{1101}$ . So, if this distance is measured, the energy difference  $\Delta E_{1101}$  can be obtained. Furthermore, as the CQW's radius increases the difference between two energy levels ( $\Delta E_{1101}$ ) decreases, so the first and the third peaks shift to the second one as seen in the figure. As  $R$  becomes infinite (bulk semiconductor), the first and the third peaks are disappeared. In the following, we will use the third peak of each curve to investigate the influence of the phonon confinement on the LWs of ODEPR peaks. To do this we plot the dependence of the AP on the photon energy for both models: the bulk-phonon (3D) and the confined-phonon models.

In Fig. 2 we can see that all the peaks in the case of bulk phonons are located at the photon energy of 55.4730 meV while the peaks in the case of confined-phonon absorption are at the



**Fig. 3.** Comparison of the LW in the GaAs/AlAs CQW of  $R=16$  nm between the cases of bulk phonons (the closed squares) and confined phonons (the closed circles).

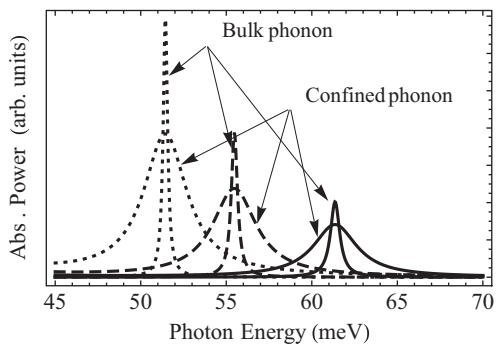


**Fig. 4.** The AP as a function of the photon energy in GaAs/AlAs CQW at  $T=250$  K for two models of phonon; the solid, the dashed, and the dotted curves correspond to radius  $R=14$  nm, 16 nm, and 18 nm, respectively.

photon energy of 55.4728 meV. The difference between these two values is seen not to be considerable and can be neglected. Thus, the phonon confinement effect does not have an effect on the peak location of the ODEPR. The appearances of resonant peaks at the same value of the photon energy also show that the ODEPR does not depend on the temperature. However, the influence of the phonon confinement is much more considerable when we consider the LW. It is easy to see that the LWs in the case of confined phonons are larger than they are in the case of bulk phonons. However, a detailed evaluation can be performed by using the profile method. This is a method of determining the LW based on graphs of the AP versus the photon energy with the help of a computational program. It was suggested by our group and has been applied successfully in some of our recent works [30–32]. Utilizing this method we obtain the dependence of the LW on the temperature as shown in Fig. 3. From Fig. 3 we can see that the LW increases with increasing temperature in both models of phonon (the bulk-phonon and confined-phonon models). Physically, this is reasonable because the possibility of the electron–phonon scattering rises as the temperature increases. It is also seen that the LW for confined phonons are larger than they are for the corresponding bulk phonons. This means that phonon confinement gives rise to the possibility of the electron–phonon scattering.

In Fig. 4, the AP is plotted versus the photon energy for the two above-mentioned models of phonons at the different values of the wire's radius. From the figure, we can see that the resonant peaks shift to smaller photon energy when the wire's radius increases. The appearance of these peaks can be explained by using the ODEPR condition, as shown above in Fig. 1. For each value of the photon energy at the resonance, the LW for confined phonons is always larger than it is for the corresponding bulk phonons. A detailed consideration based on the profile method is shown in Fig. 5 where we plot the dependence of the LW on the wire's

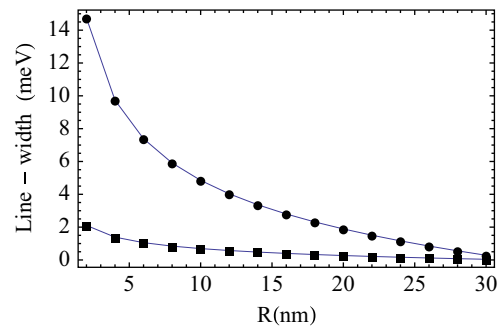


**Fig. 5.** Comparison of the LW in GaAs/AlAs CQW at  $T=250$  K between the cases of bulk phonons (the closed squares) and confined phonons (the closed circles).

radius. From Fig. 5, we can see that the LW decreases with increasing wire's radius for both models of the phonon. The result is consistent with that shown in some previous works [2,8,9]. This can be explained physically by a decrease in the possibility of electron–phonon scattering when the wire's radius increases. Furthermore, the LW for the confined-phonon case varies faster and has a larger value than it does for the bulk-phonon case, and the smaller the wire's radius is, the more pronounced the difference is. Thus, as the wire's radius decreases, the phonon confinement becomes more important and cannot be neglected. For wires with radii larger than 30 nm, the influence of phonon confinement on the LW is very small and can be ignored.

#### 4. Conclusions

In the present paper, we have calculated analytical expressions for the conductivity tensor and the AP in CQWs due to confined electron–confined-LO phonon interaction. From the graphs of the AP, we obtained the LW as a profile of curves. Computational results show that in the cases of both bulk and confined phonons, the LW increases with increasing temperature and decreases with increasing the wire's radius. In addition, the value of the LW in the case of confined phonons is greater than and asymptotic to that in the case of bulk phonons when  $R$  increases. However, for wires with radii larger than 30 nm, the influence of the phonon confinement on the LW is very small and can be ignored. This result is the same as that obtained in a two-dimensional system which is verified by theory and experiments.

#### References

- [1] J.M. Miloszewski, M.S. Wartak, P. Weetman, O. Hess, *Journal of Applied Physics* 106 (2009) 063102.
- [2] H.N. Spector, J. Lee, P. Melman, *Physical Review B* 34 (1986) 2554.
- [3] S.H. Park, S.L. Chuang, *Applied Physics A* 78 (2004) 107.
- [4] S. Melnik, G. Huyet, A.V. Uskov, *Optics Express* 14 (2006) 2950.
- [5] F. Zhang, L. Li, X.H. Ma, Z.G. Li, Q.X. Sui, X. Gao, Y. Qu, B.X. Bo, G.J. Liu, *Acta Physica Sinica* 61 (2012) 054209.
- [6] P.K. Kondratko, S.L. Chuang, G. Walter, T. Chung, N. Holonyak, *Applied Physics Letters* 83 (2003) 4818.
- [7] H. Weman, L. Sirigu, K.F. Karlsson, K. Leifer, A. Rudra, E. Kapon, *Applied Physics Letters* 81 (2002) 2839.
- [8] H. Ham, H.N. Spector, *Physical Review B* 62 (2000) 13599.
- [9] H. Ham, H.N. Spector, *Journal of Applied Physics* 90 (2001) 2781.
- [10] W.H. Seo, B.H. Han, *Solid State Communications* 119 (2001) 367.
- [11] C. Matthiesen, A.N. Vamivakas, M. Atatüre, *Physical Review Letters* 108 (2012) 093602.
- [12] C.Y. Lin, F. Grillo, N.A. Naderi, Y. Li, L.F. Lester, *Applied Physics Letters* 96 (2010) 051118.
- [13] K.C. Kim, I.K. Han, J.I. Lee, T.G. Kim, *Nanotechnology* 21 (2010) 134010.
- [14] A. Ulhaq, S. Ates, S. Weiler, S.M. Ulrich, S. Reitzenstein, A. Löffler, S. Höfling, L. Worschech, A. Forchel, P. Michler, *Physical Review B* 82 (2010) 045307.
- [15] F.X. Peng, M.J. Hai, L.X. Jin, X.G. Yong, Z.H. Yong, Y. Tao, *Optics Letters* 37 (2012) 1298.
- [16] C.R. Bennett, K. Guven, B. Tanatar, *Physical Review B* 57 (1998) 3994.

- [17] SeGi Yu, K.W. Kim, M.A. Strosio, G.J. Iafrate, A. Ballato, *Physical Review B* 50 (1994) 1733.
- [18] N. Bannov, V. Aristov, V. Mitin, M.A. Strosio, *Physical Review B* 51 (1995) 9930.
- [19] N. Nishiguchi, *Physical Review B* 52 (1995) 5279.
- [20] A. Svizhenko, A. Balandin, S. Bandyopadhyay, M.A. Strosio, *Physical Review B* 57 (1998) 4687.
- [21] Ka-Di Zhu, Shi-Wei Gu, *Solid State Communications* 89 (1994) 151.
- [22] G. Fasol, M. Tanaka, H. Sakaki, Y. Horikoshi, *Physical Review B* 38 (1988) 6056.
- [23] A.K. Sood, J. Menendez, M. Cardona, K. Ploog, *Physical Review Letters* 54 (1985) 2111.
- [24] M.A. Strosio, *Physical Review B* 40 (1989) 6428; M.V. Klein, *Journal of Quantum Electronics* QE-22 (1986) 1760.
- [25] J.K. Jain, S. Das Sarma, *Physical Review Letters* 62 (1989) 2305.
- [26] B.K. Ridley, *Physical Review B* 39 (1989) 5282.
- [27] S. Rudin, T.L. Reinecke, *Physical Review B* 41 (1990) 7713.
- [28] D. Dunn, A. Suzuki, *Physical Review B* 29 (1984) 942.
- [29] Y.J. Cho, S.D. Choi, *Physical Review B* 49 (1994) 14301.
- [30] T.C. Phong, H.V. Phuc, *Modern Physics Letters B* 25 (2011) 1003.
- [31] T.C. Phong, L.T.T. Phuong, H.V. Phuc, *Superlattices and Microstructures* 52 (2012) 16.
- [32] H.V. Phuc, L. Dinh, T.C. Phong, *Journal of the Korean Physical Society* 60 (2012) 1381.
- [33] X.F. Wang, X.L. Lei, *Physical Review B* 49 7 (1994) 4780.
- [34] N.L. Kang, S.D. Choi, *Journal of the Physical Society of Japan* 78 2 (2009) 0247101.
- [35] N.L. Kang, S.D. Choi, *Journal of the Korean Physical Society* 44 (2004) 938.
- [36] H.J. Lee, N.L. Kang, J.Y. Sug, S.D. Choi, *Physical Review B* 65 (2002) 195113.
- [37] M. Masale, N.C. Constantious, *Physical Review B* 48 (1993) 11128.
- [38] A. Gold, A. Ghazali, *Physical Review B* 41 (1990) 7626.
- [39] N.C. Constantiou, B.K. Ridley, *Physical Review B* 41 (1990) 10622.
- [40] Y.B. Yu, Sh.N. Zhu, K.X. Gu, *Solid State Communications* 139 (2006) 76.
- [41] N.C. Constantious, B.K. Ridley, *Physical Review B* 41 (15) (1989) 10627.
- [42] S.C. Lee, *Journal of the Korean Physical Society* 52 (2008) 1832.
- [43] S.C. Lee, J.W. Kang, H.S. Ahn, M. Yang, N.L. Kang, S.W. Kim, *Physica E* 28 (2005) 402.